CrossMark

ORIGINAL PAPER

# Under-ice distribution of polar cod *Boreogadus saida* in the central Arctic Ocean and their association with sea-ice habitat properties

Carmen David[1,2] · Benjamin Lange[1,2] · Thomas Krumpen[1] · Fokje Schaafsma[3] ·
Jan Andries van Franeker[3] · Hauke Flores[1,2]

**Abstract** In the Arctic Ocean, sea-ice habitats are undergoing rapid environmental change. Polar cod (*Boreogadus saida*) is the most abundant fish known to reside under the pack-ice. The under-ice distribution, association with sea-ice habitat properties and origins of polar cod in the central Arctic Ocean, however, are largely unknown. During the RV *Polarstern* expedition ARK XXVII/3 in the Eurasian Basin in 2012, we used for the first time in Arctic waters a Surface and Under Ice Trawl with an integrated bio-environmental sensor array. Polar cod was ubiquitous throughout the Eurasian Basin with a median abundance of 5000 ind. km$^{-2}$. The under-ice population consisted of young specimens with a total length between 52 and 140 mm, dominated by 1-year-old fish. Higher fish abundance was associated with thicker ice, higher ice coverage and lower surface salinity, or with higher densities of the ice-amphipod *Apherusa glacialis*. The fish were in good condition and well fed according to various indices. Backtracking of the sea-ice indicated that sea-ice sampled in the Amundsen Basin originated from the Laptev Sea coast, while sea-ice sampled in the Nansen Basin originated from the Kara Sea. Assuming that fish were following the ice drift, this suggests that under-ice polar cod distribution in the Eurasian Basin is dependent on the coastal populations where the sea-ice originates. The omnipresence of polar cod in the Eurasian Basin, in a good body condition, suggests that the central Arctic under-ice habitats may constitute a favourable environment for this species survival, a potential vector of genetic exchange and a recruitment source for coastal populations around the Arctic Ocean.

This article belongs to the special issue on the "Ecology of Arctic Gadids", coordinated by Franz Mueter, Jasmine Nahrgang, John Nelson and Jørgen Berge.

✉ Carmen David
  Carmen.David@awi.de

[1] Alfred Wegener Institut Helmholtz-Zentrum für Polar- und Meeresforschung, Am Handelshafen 12, 27570 Bremerhaven, Germany

[2] Centre for Natural History (CeNak), Zoological Museum, University of Hamburg, Martin-Luther-King Platz 3, 20146 Hamburg, Germany

[3] IMARES Wageningen UR, PO Box 167, 1790 AD Den Burg (Texel), The Netherlands

## Introduction

The Arctic Ocean is facing some of the most pronounced effects of global climate change (IPCC 2014). During the past four decades, the Arctic Ocean has experienced lengthening of the melt season and a progressive reduction in sea-ice extent and thickness (Rigor and Wallace 2004; Shimada et al. 2006; Kwok and Rothrock 2009; Markus et al. 2009; Stroeve et al. 2012). Sea-ice decline is expected to have a direct impact on organisms living in association with the sea-ice.

Polar cod (*Boreogadus saida*) is the most abundant Arctic fish that resides under the pack-ice (Lønne and Gulliksen 1989; Gradinger and Bluhm 2004). The pack-ice serves as habitat for an unknown part of the first- and second-year polar cod population (Lønne and Gulliksen 1989), while large populations are widespread around the

Arctic shelves. Polar cod is considered an ecological key species in the Arctic Ocean due to its pan-Arctic distribution (Bouchard and Fortier 2011), large standing stocks (Geoffroy et al. 2011; Hop and Gjøsæter 2013) and its role as an energy transmitter to higher trophic levels (Welch et al. 1992; Hop et al. 1997a; Harter et al. 2013), Along the Arctic shelves, polar cod are often recorded below sea-ice in autumn and winter (Benoit et al. 2008; Geoffroy et al. 2011). According to Welch et al. (1993), the sea-ice may offer protection against marine mammals and predatory sea birds for which polar cod is known to be an important food source (Bradstreet and Cross 1982; Lønne and Gabrielsen 1992; Welch et al. 1992; Haug et al. 2007). When the ice melts, they become part of the bentho-pelagic stock (Falk-Petersen et al. 1986; Hop et al. 1997b; Hop and Gjøsæter 2013). High polar cod aggregations were reported in the presence of ice cover during winter in the Amundsen Gulf (Geoffroy et al. 2011), where estimated fish biomass reached 250 kt (Benoit et al. 2014). During the open water season, large schools of polar cod were reported from the Barrow Strait reaching up to 12,000 t per school and Lancaster Region up to 75,000 t per school (Welch et al. 1992). The only population, regularly monitored, persists in the Barents Sea, where the largest known standing stock of polar cod, up to 1.5 million t, exists (Hop and Gjøsæter 2013).

These high fish stock areas are believed to be important reproduction grounds for the polar cod. Reproduction success is related to sea-ice extent and duration, i.e. timing of ice break-up and freezing, and the formation of early polynyas (Fortier et al. 2006; Bouchard and Fortier 2008, 2011). At the onset of winter, older polar cod follow the downward migration of zooplankton (Geoffroy et al. 2011), while larvae and young juveniles aggregate in the surface layer (Benoit et al. 2014; Geoffroy et al. in press). A part of the young polar cod remaining in the surface layer probably associates with the drifting sea-ice and is carried away from the shelves, as young polar cod were frequently observed and sampled in drifting sea-ice by divers (Lønne and Gulliksen 1989; Søreide et al. 2006). Many uncertainties regarding this behaviour remain to be elucidated. Observations by divers provided great insights into the under-ice behaviour of young polar cod. It was reported that narrow wedges of seawater along the edges of ice floes provide microhabitats for polar cod inhabiting sea-ice over the deep basins (Gradinger and Bluhm 2004). Sea-ice habitat structure might, therefore, have a big impact on young polar cod survival. Yet no detailed studies have quantified the association of young polar cod with sea-ice habitat properties on large spatial scales. The few existing estimates are based on localised under-ice observations which do not reflect continuous environmental gradients, but rather exceptional events, e.g. calm weather conditions versus storms (Melnikov and Chernova 2013) or contrasting sea-ice structure, e.g. flat versus rafted ice (Lønne and Gulliksen 1989; Gradinger and Bluhm 2004). This demonstrates a strong need for extended information regarding larger-scale distribution patterns of under-ice polar cod and the condition of these fish in order to better understand this trait of polar cod's life history and implications for ecosystem functioning. A new sampling gear previously deployed in the Southern Ocean, the Surface and Under Ice Trawl (SUIT; van Franeker et al. 2009), can overcome the spatial limitation of observations by divers (Flores et al. 2012) by enabling large-scale horizontal sampling of the 0-2 m surface layer, both under sea-ice and in open water.

This study focuses on polar cod sampled with SUIT, during summer 2012, under pack-ice within the Eurasian sector of the central Arctic Ocean. The specific objectives are: (1) to investigate the under-ice distribution, population structure and physiological condition of polar cod in the Eurasian Basin, (2) to analyse the association of polar cod abundance with sea-ice habitat properties and (3) to identify regions of origin where young polar cod found in the central Arctic Ocean might have entered the under-ice habitat.

## Methods

### Sampling technique and data collection

Polar cod were sampled during the RV *Polarstern* expedition "IceArc" (ARK XXVII/3). Sampling was performed between 2 August and 29 September 2012 across the Eurasian sector of the central Arctic Ocean (Fig. 1). Thirteen horizontal hauls were performed under different sea-ice types (multi-year ice, first-year ice) and degrees of ice coverage. Nine stations were positioned nearby representatively selected multi-disciplinary sea-ice stations (Boetius et al. 2013) to ensure comparability of parameters. The remaining four stations were completed at intermediate positions to maximise the coverage of the investigation area. Sampling was performed by horizontal trawling with a SUIT (van Franeker et al. 2009). The SUIT consisted of a steel frame with a 2 m × 2 m opening and 2 parallel 15-m-long nets attached: (1) a 7-mm half-mesh commercial shrimp net, lined with 0.3-mm mesh in the rear 3 m of the net, covered 1.5 m of the opening width and (2) a 0.3-mm mesh zooplankton net, covered 0.5 m of the opening width. Floats attached to the top of the frame kept the net at the surface or the sea-ice underside. To enable sampling under undisturbed ice, an asymmetric bridle forces the net to tow at an angle of approximately 60° starboard of the ship's track, at a cable length of 150 m. A detailed description of
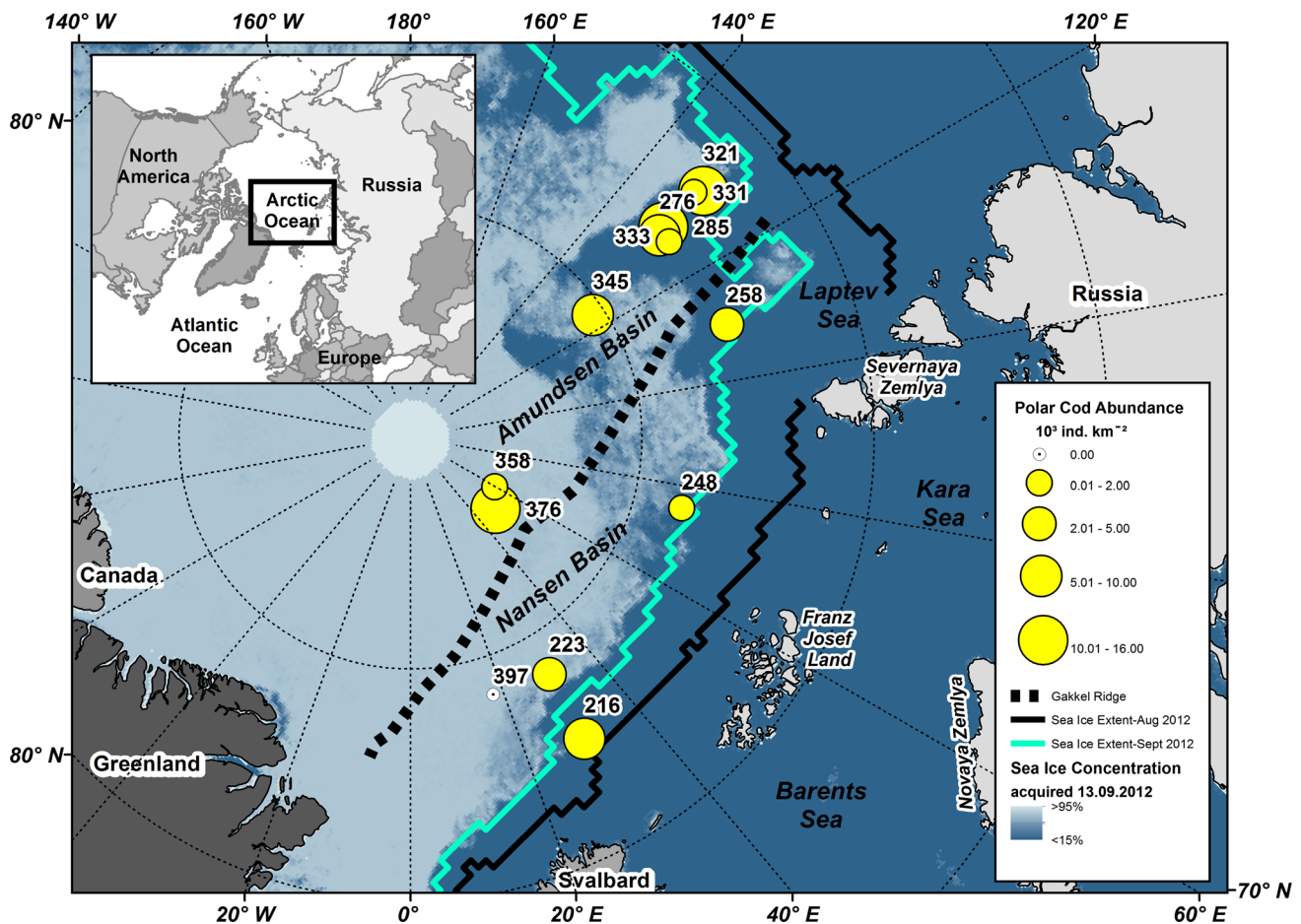
**Fig. 1** Station map during RV Polarstern expedition IceArc (ARK XXVII/3) and polar cod abundance. Sea-ice concentration on 13 September 2012 (data acquired from Bremen University, http://www.iup.uni-bremen.de:8084/amsr/) and monthly mean sea-ice extent for August and September 2012 are represented on the map (data acquired from NSIDC, Fetterer et al. 2002, daily updated). *Number codes* next to sampling locations indicate station numbers

the SUIT construction and sampling performance is provided as supplementary material in Flores et al. (2012). Depending on the ice conditions, SUIT haul durations varied between 3 and 38 min, with a mean of 24 min, over a mean sampled distance of about 1.3 km (Table 2). A bio-environmental sensor array was mounted in the SUIT frame, consisting of an acoustic Doppler current profiler, a conductivity-temperature-depth (CTD) probe with built-in fluorometer and altimeter, two spectral radiometers and a video camera. A detailed description of environmental data acquisition is provided in David et al. (2015).

A CTD probe with a carousel water sampler was used to collect environmental parameters from the water column near SUIT stations (David et al. 2015). The depth of the upper mixed layer was calculated from the ship CTD profiles after Shaw et al. (2009). Details of the CTD sampling procedure and nutrients analysis were provided in Boetius et al. (2013). Data are available online in the PANGAEA database (Rabe et al. 2012).

## Sea-ice back-tracking

To determine the pathways and formation areas of sampled sea-ice, we back-tracked the sampled sea-ice areas over a period of 2 years, using sea-ice drift and concentration data from passive microwave satellite sensors. Passive microwave-based ice drift products were provided by different institutions and have been widely used in sea-ice studies and for model assimilation. The motion fields provided by the Centre for Satellite Exploitation and Research (CERSAT) at the Institut Francais de Recherche pour d'Exploitation de la Mer (IFREMER), France (hereafter referred to as CERSAT), are based on a combination of drift vectors estimated from scatterometer (SeaWinds/QuikSCAT and ASCAT/MetOp) and radiometer (SSM/I) data. They are available with a grid size of 62.5 km, using time lags of 3 days for the period between September and May. Hence, during the winter month, the ice drift data provided by CERSAT were used in the tracking approach.

Because of its year-round availability, Polar Pathfinder sea-ice Motion Vectors (version 2), provided by the National Snow and Ice Data Centre (NSIDC, Boulder, USA), were used for the calculation of ice pathways and sources during summer months. The product contains daily gridded fields of sea-ice motion on a 25-km Equal-Area Scalable Earth grid (Fowler et al. 2013). The motion vectors are obtained from a variety of satellite-based sensors such as the SMMR, SSM/I, AMSR-E and Advanced Very High Resolution Radiometer, and buoy observations from the International Arctic Buoy Program. A description of the dataset and the sea-ice motions retrieval algorithm can be found in Fowler et al. (2013). Sea-ice concentration data used in this study were also provided by the NSIDC. Data are calculated based on the Advanced Microwave Scanning (AMSR-E) Bootstrap Algorithm and available on a daily basis, with a $25 \times 25$ km spatial resolution (Fowler et al. 2013). Eurasian Basin sea-ice-covered area, as monthly means for August and September 2012, was estimated in ArcGIS 10.1 using sea-ice extent data provided by the NSIDC (Fetterer et al. 2002, updated daily), defining a sea-ice concentration of 15 % as the boundary between sea-ice and open water. Lambert Azimuthal equal area was used as projection system because it realistically preserves the area (Snyder 1992). During back-tracking, a specific particle is followed backward in time until: (a) the ice particle approaches land, (b) the sea-ice concentration at the position of the particle reaches a critical value (<15 %) and the ice is assumed to be melted, or (c) the tracking time of 2 years is exceeded.

## Fish processing

Immediately after sampling, fish were frozen at −20 °C. Before freezing, several fish were sampled for lipid and stable isotopes analyses and stomach content (data not included in this study). At the Alfred Wegener Institute, frozen fish were first thawed and then blotted dry before further analysis. Total length (TL) and standard length (SL) were measured to the lowest full mm. Total wet weight (WW) and eviscerated wet weight (EWW) were recorded to the nearest 0.1 mg. Liver and gonads weight were determined to the nearest 0.01 mg. Otoliths (sagittae) were extracted. Otolith length (OL) was determined using a Leica 21.5 M stereomicroscope equipped with a camera and Leica LAS V4.1 image analysis software.

Among the measured (TL, SL) and weighted (WW) fish, a random selection of ten fish (from three stations with the highest catches) was processed for energy content estimation. These fish were freeze-dried until complete desiccation (constant mass). After drying, they were re-weighed to determine the total dry weight (DW). Water content was calculated as the difference between WW and DW,

expressed as %WW. Then, fish were homogenised with a blender. A subsample of each fish of approximately 0.5 g was used for calorimetry. Individual energy content, expressed as kJ/g, was determined at the Royal Netherlands Institute for Sea Research (NIOZ) with an isoperibol bomb calorimeter (IKA C2000 basic) calibrated with benzoic acid.

## Data analysis

Pairwise linear regressions were applied between TL, SL, WW, EWW and OL. To describe the condition of fish, a set of indices were estimated: Fulton's condition index ($K = 100 \times WW/TL^3$), condition index (CI = $100 \times EWW/WW$), hepatosomatic index ($100 \times$ liver weight/WW) and gonadosomatic index ($100 \times$ gonads weight/WW). To assess the statistical difference between basins and areas of sea-ice formation, the Wilcoxon signed-rank test was performed on fish abundance data and condition indices (Wilcoxon 1945).

Generalised linear models (McCullagh and Nelder 1989) were used to analyse the relationship of polar cod abundance with sea-ice habitat properties. Eight environmental variables were selected a priori, from a suite of 30 variables obtained during sampling (Online resource 1), by Spearman's rank correlation coefficient, used to identify redundant variables. In pairs with correlation higher than 0.7, only one variable was chosen for subsequent analysis based on the ecological relevance to the objectives of this study, and model requirements, e.g. normality of data. In a second approach, four biological variables (zooplankton species densities, representing potential prey of polar cod, caught during the same trawls), were additionally used for statistical modelling (Table 1). Zooplankton data collection is described in David et al. (2015). Data were checked for normality by histograms, Shapiro tests and QQ plots. To obtain an even distribution of residuals, two environmental variables were transformed: proportional ice coverage during SUIT hauls ('coverage') by square-power transformation and nitrate + nitrite (NOx) by square-root transformation. The biological variables were log-transformed. The response variable, polar cod abundance was square-root-transformed.

Two full models were submitted to model selection: (1) a model containing all physical and biological variables and (2) a model containing only physical variables (Table 1). Two stations, from which no quantitative prey abundance data were available, were excluded from model (1). An automatic backwards selection, using the Akaike information criterion (AIC), was applied for selection of the most parsimonious model. Since this method can result in over-fitted models (Vaz et al. 2008), alternatively simple models containing just one variable, one variable and its

**Table 1** Environmental and biological variables characterising sea-ice habitats selected for statistical modelling

| Station code<br>Basin | 216<br>Nansen | 223<br>Nansen | 248<br>Nansen | 258<br>Nansen | 276<br>Amundsen | 285<br>Amundsen | 321<br>Amundsen | 331<br>Amundsen | 333<br>Amundsen | 345<br>Amundsen | 358<br>Amundsen | 376<br>Amundsen | 397<br>Nansen |
|---|---|---|---|---|---|---|---|---|---|---|---|---|---|
| Coverage (%) | 98.3 | 81.5 | 56.4 | 100 | 78.7 | 100 | 63.8 | 0.0 | 4.0 | 62.3 | 85.8 | 100 | 96.2 |
| Thickness (m) | 0.45 | 1.15 | 1.14 | 0.75 | 0.85 | 0.85 | 0.55 | 0.00 | 0.00 | 1.05 | 1.38 | 1.40 | 0.70 |
| Roughness | 0.15 | 0.34 | 0.34 | 0.06 | 0.18 | 0.15 | 0.48 | 0.00 | 0.00 | 0.24 | 0.14 | 0.49 | 0.39 |
| Temperature (°C) | −1.06 | −1.51 | −1.55 | −1.61 | −1.42 | −1.56 | −1.61 | −1.58 | −1.22 | −1.60 | −1.81 | −1.82 | −1.76 |
| Salinity | 30.9 | 31.8 | 32.2 | 32.6 | 30.2 | 30.6 | 29.4 | 30.4 | 30.1 | 30.1 | 33.1 | 33.1 | 32.6 |
| MLD (m) | 9 | 15 | 18 | 15 | 22 | 22 | 20 | 20 | 20 | 25 | 30 | 25 | 22 |
| Chlorophyll $a$ (mg m$^{-3}$) | 0.29 | 0.20 | 0.27 | 0.15 | 0.26 | 0.32 | 0.35 | 0.36 | 0.19 | 0.44 | 0.32 | 0.28 | 0.24 |
| NOx (µmol l$^{-1}$) | 6.21 | 4.63 | 6.84 | 1.56 | 2.42 | 2.42 | 0.12 | 0.12 | 1.10 | 0.50 | 1.26 | 3.01 | 3.46 |
| *Apherusa glacialis* (ind. 1000 m$^{-2}$) | 195.10 | 2218.44 | 152.67 | 502.24 | 823.16 | 1906.75 | 349.86 | 136.84 | 44.12 | 342.66 | na | na | 162.97 |
| *Themisto libellula* (ind.1000 m$^{-2}$) | 9.46 | 7.11 | 3.80 | 30.38 | 87.10 | 853.57 | 512.33 | 310.07 | 345.23 | 260.05 | na | na | 6.11 |
| *Calanus glacialis* (ind. 1000 m$^{-2}$) | 37.85 | 1911.27 | 30,528.14 | 4146.93 | 1177.70 | 2216.59 | 184.62 | 154.31 | 498.49 | 178.16 | na | na | 1124.51 |
| *Calanus hyperboreus* (ind. 1000 m$^{-2}$) | 41.45 | 3697.39 | 4946.13 | 555.57 | 471.08 | 309.85 | 29.54 | 11.65 | 74.31 | 0.00 | na | na | 65.19 |

Abbreviations used in the text and figures are indicated in parentheses: sampled ice coverage during SUIT hauls (coverage), modal ice thickness (thickness), roughness of ice thickness (roughness), surface water temperature (temperature), surface water salinity (salinity), chlorophyll $a$ concentration at the surface (chlorophyll $a$), combined nitrate + nitrite concentration at the depth of the chlorophyll $a$ maximum (NOx), mixed-layer depth (MLD)

quadratic term, combinations of two and three variables, simple or with interactions were fitted. The resulting models were further compared based on AIC, adjusted R-squared and dispersion. The significance of model improvement by AIC was confirmed with ANOVA statistics.

For all analyses, R software version 3.2.0 (R Core Team 2015) was used with the libraries vegan, FactoMineR, plyr, MASS, mixtools and modEvA.

## Results

### Sea-ice habitat properties and sea-ice back-tracking

Across the Eurasian Basin, 13 stations were sampled (Fig. 1). Five stations were located in the Nansen Basin and eight stations in the Amundsen Basin. Four of the Nansen Basin stations were sampled during the first half of August and the Amundsen Basin stations during late

August to mid-September. The last station (Stn 397) was sampled in the Nansen Basin on 29 September 2012, at the onset of winter. Two of the Amundsen Basin stations were nearly ice-free. At all other stations, sea-ice was present, with concentrations ranging from 56 to 100 % (Table 1). Modal ice thickness ranged from 0.45 to 1.40 m. Surface water temperatures ranged between −1.8 and −1.0 °C. Surface water salinity was significantly higher in the Nansen Basin (30–33) than in the Amundsen Basin (29–31) ($W = 0$, $p$ value <0.01). A detailed description of the above-mentioned physical properties of the study region is provided in David et al. (2015).

Thirteen areas of sea-ice, corresponding to the ice sampled during each SUIT station, were back-tracked to their area of ice formation (Fig. 2; Table 2). We found that most of the ice originated from shallow coastal areas, where ice is formed in polynyas situated along the fast ice edge. A minor part was formed during freeze-up and in deeper waters (>200 m). Sea-ice from all stations sampled in the Nansen Basin originated from the Kara Sea sector
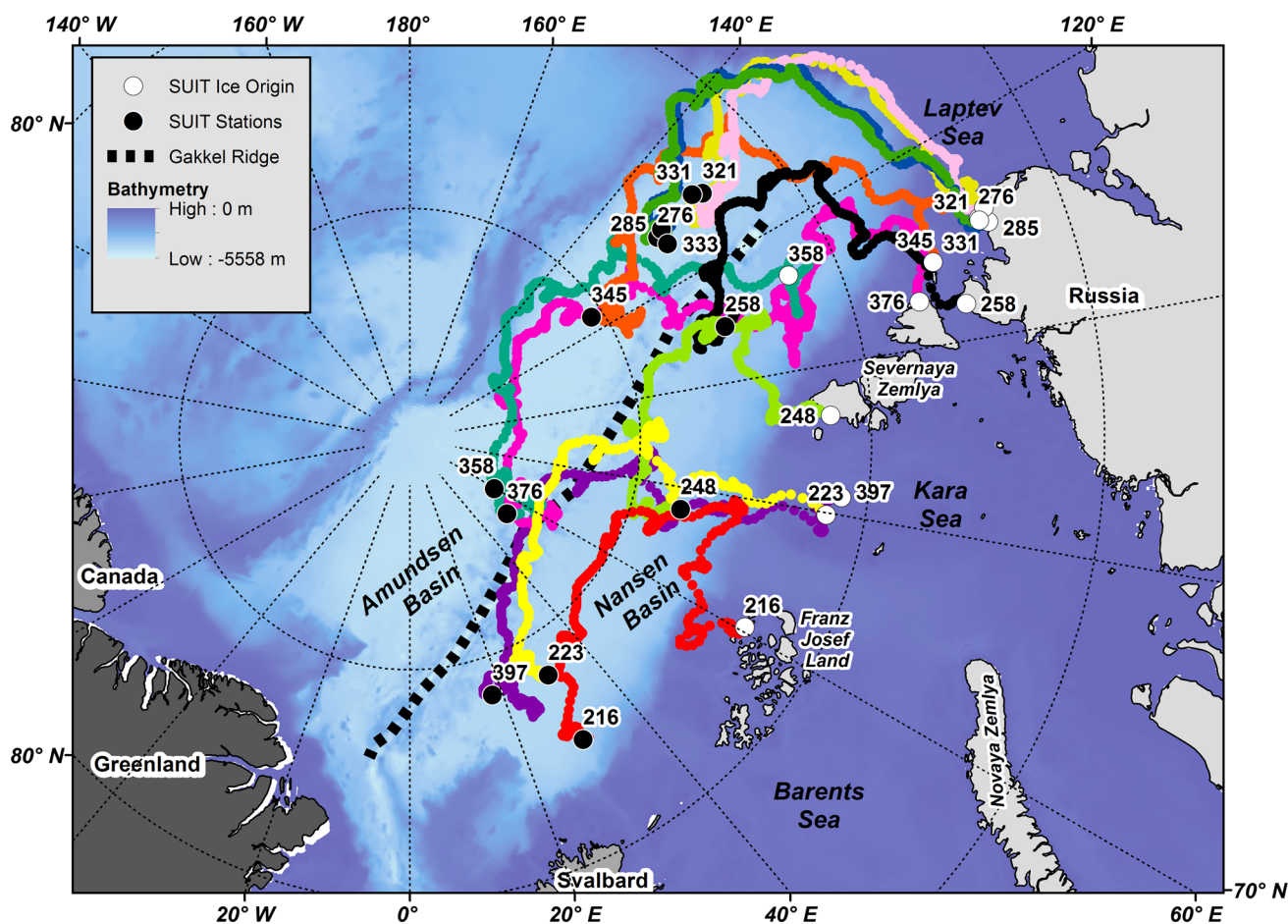


**Fig. 2** *Back*-tracked drift pathways of sea-ice at SUIT sampling locations, during RV Polarstern expedition IceArc (ARK XXVII/3). *Black circles* represent the SUIT station locations. *White circles* represent the likely formation areas of sampled sea-ice. *Number codes* next to formation areas and sampling locations indicate corresponding SUIT station numbers

**Table 2** Summary of sampled sea-ice area drift characteristics and polar cod abundance at each corresponding SUIT station

| Station code | SUIT | | | | Sea-ice drift | | Sea-ice origin | | | | |
|---|---|---|---|---|---|---|---|---|---|---|---|
| | Latitude (°N) | Longitude (°E) | Trawled distance (m) | Fish abundance ($10^3$ ind. km$^{-2}$) | Drift duration (days) | Drift distance (km) | Latitude (°N) | Longitude (°E) | Depth (m) | Formation date | Area |
| 216 | 82.50 | 30.00 | 2219 | 5.85 | 240 | 2113 | 81.68 | 60.72 | 200 | 11 Dec | Kara Sea |
| 223 | 84.07 | 30.12 | 703 | 4.97 | 261 | 2056 | 80.83 | 79.71 | 100 | 22 Nov | Kara Sea |
| 248 | 83.97 | 75.80 | 1578 | 0.63 | 249 | 1795 | 80.87 | 93.20 | 0 | 11 Dec | Kara Sea |
| 258 | 82.71 | 109.53 | 1613 | 2.48 | 269 | 1985 | 77.62 | 103.66 | 0 | 25 Nov | Kara Sea |
| 276 | 83.06 | 129.76 | 1630 | 7.36 | 269 | 1998 | 76.81 | 111.22 | 100 | 30 Nov | Laptev Sea |
| 285 | 82.91 | 129.76 | 1342 | 10.05 | 271 | 2004 | 76.64 | 110.57 | 0 | 29 Nov | Laptev Sea |
| 321 | 81.68 | 129.79 | 1083 | 11.54 | 255 | 1868 | 76.62 | 111.97 | 0 | 24 Dec | Laptev Sea |
| 331 | 81.90 | 130.59 | 1374 | 0.36 | 276 | 1975 | 76.81 | 110.99 | 100 | 4 Dec | Laptev Sea |
| 333 | 83.03 | 127.05 | 1292 | 0.77 | na | na | na | na | na | na | na |
| 345 | 85.16 | 122.59 | 1392 | 8.98 | 321 | 2358 | 78.05 | 108.66 | 100 | 24 Oct | Laptev Sea |
| 358 | 87.86 | 60.67 | 1476 | 0.67 | 343 | 2546 | 81.06 | 113.36 | 2000 | 12 Oct | Laptev Sea |
| 376 | 87.42 | 52.90 | 125 | 15.92 | 618 | 4248 | 78.58 | 105.08 | 0 | 16 Jan | Laptev Sea |
| 397 | 84.19 | 17.41 | 982 | 0 | 333 | 2594 | 80.57 | 82.33 | 200 | 1 Nov | Kara Sea |

(Fig. 2). At Stn 216, the ice originated from the coast of Franz Josef Land. At the Gakkel ridge station (Stn 258), the ice originated from the coast of Severnaya Zemlya, bordering the Kara Sea sector. At all of the Amundsen Basin stations, the sampled sea-ice originated from the Laptev Sea coast, east of Severnaya Zemlya (Fig. 2). The mean drift duration of the sampled sea-ice was 308 days, with a range of 240 to 618 days (Table 2). Shorter drift durations (240 and 249 days) were determined for the sampled sea-ice areas at Stns 216 and 248 in the Nansen Basin. The longest drift duration was determined for the sampled sea-ice area at Stn 376 in the Amundsen Basin.

## Abundance, population structure and biomass distribution of polar cod

Polar cod abundance in the 0-2 m surface layer ranged between 0 and 15,920 ind. km$^{-2}$ (median = 4977, SD = 5130) (Fig. 1; Table 2). The highest abundance was encountered at Stn 376 in the Amundsen Basin. The total number of fish caught at each station ranged between 0 and 28. Only at the early winter Stn 397, no fish were caught. One and two fish were caught at the open water stations, Stns 331 and 333, respectively.

The median polar cod abundance was higher in the Amundsen Basin than in the Nansen Basin (Fig. 1), coinciding with a tendency to higher abundances under sea-ice originating from the Laptev Sea compared to sea-ice formed in the Kara Sea (Fig. 2). When the two open water stations in the Amundsen Basin were excluded from analysis, this pattern was statistically significant ($W = 27$; $p < 0.05$) (Fig. 3).

The most parsimonious model, using polar cod abundance as a response variable, showed a strong positive relationship of fish abundance with surface salinity ($p < 0.01$) and the abundance of the ice-amphipod *A. glacialis* ($p < 0.01$) (Adj. $R^2 = 0.72$, AIC = 25) (Table 3). When only physical variables were included as predictors, the most parsimonious model showed a negative effect of surface salinity ($p < 0.01$) and a positive effect of sea-ice thickness ($p < 0.05$) and coverage ($p < 0.1$) on modelled fish abundance (Adj. $R^2 = 0.56$, AIC = 37) (Table 3). Details on model results are presented in Online Resource 2.

The TL of polar cod caught ranged between 52 and 140 mm (Fig. 4). Fish in the Nansen Basin were significantly larger than fish in the Amundsen Basin ($W = 911$, $p < 0.001$). This pattern was driven by the dominance of larger fish at two stations, Stns 216 and 223, having a mean TL per station of 86 and 100 mm, respectively. Two exceptionally large fish were caught, one at Stn 216 (TL = 137 mm) and one at Stn 285 (TL = 140 mm). The Nansen fish comprised only 28 % of the total catch, with a TL mode of 89 mm and a range of 56–137 mm. The Amundsen fish had a TL mode of 72 mm and a range of 52–140 mm. The mean individual fish wet weight (WW) was 4.96 g (range 1.1–18.8 g) in the Nansen Basin and 2.16 g (range 0.8–8.5 g) in the Amundsen Basin.

The total biomass per station ranged between 0 and 66 kg km$^{-2}$ (median = 19.34 kg km$^{-2}$, SD = 18.79). The highest biomass was encountered at Stn 376 in the Nansen Basin. Except Stn 397 where no fish were caught, the lowest biomass was found at the open water Stn 331, closely followed by Stns 248 and 333. Average biomass was somewhat higher in the Nansen Basin than in the
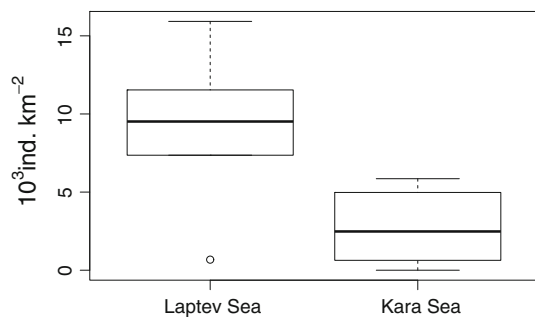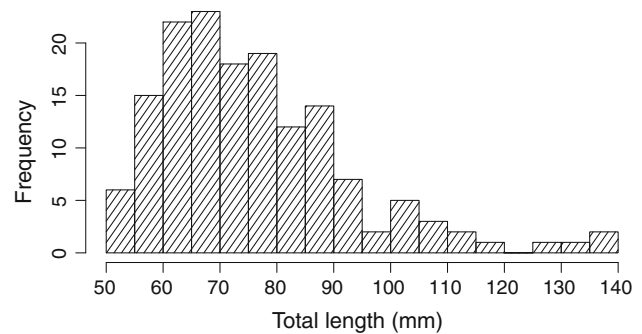
**Fig. 3** *Boxplot* of polar cod abundance at sampling stations grouped according to two main areas of sea-ice formation: Laptev Sea and Kara Sea. The *horizontal bar* indicates median abundance. The *upper* and the *lower* edges of the 'box' (hinges) denote the approximate first and third quantiles, respectively. The two open water sampling stations (Stns 331 and 333) were excluded



**Fig. 4** Histogram of the size distribution for polar cod sampled with the SUIT during RV Polarstern expedition IceArc (ARK XXVII/3)

Amundsen Basin, due to the influence of larger fish caught at Stn 216 and 223, but this pattern was not statistically significant ($W = 22$; $p > 0.1$).

### Allometrics and energy content

A summary of various allometric regression analyses was provided in Table 4. Significant positive linear relationships existed between TL and OL ($n = 130$, Adj. $R^2 = 0.94$; $p < 0.001$) and between TL and SL ($n = 130$, Adj. $R^2 = 0.99$, $p < 0.001$). WW and EWW were exponentially related to TL ($n = 127$, Adj. $R^2 = 0.96$, $p < 0.001$). The exponential regression coefficient $b$, for fish of size 52–120 mm, was 2.13 for WW estimates and 2.10 for EW estimates (Table 4).

The condition indices were analysed in 130 fish having a mean length (TL) of 76 mm and mean weight (WW) of $3.2 \pm 2.5$ g (Table 5). The condition index (CI) had a mean of 78.8 % $\pm$ 3.3. Fish from the Nansen Basin had a significantly higher CI (80 % $\pm$ 3.3) compared with fish from the Amundsen Basin (78 % $\pm$ 3.2) ($W = 10{,}793$, $p < 0.001$). Fulton's index (K) had a mean of 62.8 % $\pm$ 7.2 (Table 5). Fish from the Nansen Basin had an averaged similar K (62 % $\pm$ 6) compared with fish from

the Amundsen Basin (64 % $\pm$ 7) ($W = 1688$, $p > 0.1$). The hepatosomatic index (HSI) was significantly higher and was more variable in the Amundsen Basin (1.4 % $\pm$ 0.8) compared to the Nansen basin (1.0 % $\pm$ 0.6) ($W = 1257$, $p < 0.05$).

The ten fish from three stations (Stns 216, 285 and 321) analysed for water and energy content had a mean TL of 77.7 mm (range 60–133 mm), mean WW of 3.5 g, thus well representing the sampled population. Their mean water content was 73.2 % $\pm$ 3.1 (Table 6). The fish had a mean individual dry weight (DW) of $0.9 \pm 0.8$ g and a mean dry energy density of $27.25 \pm 1.3$ kJ /g DW (Table 6).

### Discussion

#### Under-ice distribution and association with sea-ice habitats

We used a SUIT for the first time in the Arctic Ocean, enabling us to provide the first large-scale estimates of polar cod (*B. saida*) abundance under sea-ice throughout the Eurasian Basin. When absolute fish numbers were considered per haul, our stations' catches, between 0 and 28 individuals, corresponded well with previous under-ice observations of small schools described by Gradinger and

**Table 3** Summary results of the most parsimonious models testing the association of polar cod abundance (Ab) with sea-ice habitat properties resulting from model selection

| Response variable | Overall model statistics | | Model terms | | |
|---|---|---|---|---|---|
| | | | Variables | Linear estimate | *p* value |
| Ab | Dispersion | 0.70 | Salinity | −0.9570 | 0.00413 |
| | Adj. $R^2$ | 0.56 | Thickness | 1.8270 | 0.02848 |
| | AIC | 37 | Coverage | $1.789 \times 10^{-4}$ | 0.05617 |
| Ab | Dispersion | 0.38 | Salinity | −0.6717 | 0.00511 |
| | Adj. $R^2$ | 0.72 | *A. glacialis* | 0.6788 | 0.00400 |
| | AIC | 25 | | | |

*Adj. $R^2$* adjusted R-squared, *AIC* Akaike's information criterion

**Table 4** Relationships between total body length [mm] (TL), wet weight [mg] (WW), eviscerated wet weight [mg] (EWW), otolith length [mm] (OL) and standard length [mm] (SL) for fish with a TL range of 52–120 mm

| Response variable | Regression model with coefficients | Adj. $R^2$ | $P$ value |
|---|---|---|---|
| TL | $20.6631 + OL \times 24.2791$ | $R^2 = 0.943$ | <0.001 |
| SL | $-0.2736 + 0.9187 \times TL$ | $R^2 = 0.996$ | <0.001 |
| WW | $0.0004 \times TL^{2.1305} - 1$ | $R^2 = 0.963$ | <0.001 |
| EWW | $0.0004 \times TL^{2.1073} - 1$ | $R^2 = 0.965$ | <0.001 |
| WW | $1.72E - 05 \times FL^{2.8}$[a] | na | na |

The lowermost row shows the regression model of a similar study by Matley et al. (2013) in which FL is fork length

[a] Matley et al. (2013)

**Table 5** Summary of body condition indices of all fish caught in our samples; CI—condition index; K—Fulton's condition index; HSI—hepatosomatic index; GSI—gonadosomatic index; standard deviations are provided in parentheses

| Total length (mm) | Wet weight (g) | CI (%) | $K$ (%) | HSI (%) | GSI (%) |
|---|---|---|---|---|---|
| 76.8 (16.6) $n = 130$ | 3.27 (2.5) $n = 127$ | 78.8 (3.5) $n = 127$ | 62.8 (7.2) $n = 127$ | 1.3 (0.8) $n = 96$ | 3.8 (1.8) $n = 114$ |

**Table 6** Mean total body length, wet weight, dry weight and energy content of polar cod ($n = 10$); standard deviations are provided in parentheses

| Total length (mm) | Wet weight (g) | Water content (%) | Dry weight (g) | Calorie content (Cal/g) | Energy content (kJ/g) |
|---|---|---|---|---|---|
| 77.7 (20.8) | 3.5 (3.8) | 73.2 (3.1) | 0.9 (0.8) | 6511 (316) | 27.2 (1.3) |

Bluhm (2004). At a median 5000 ind. km$^{-2}$ over the sampling area, our abundances were low compared to coastal areas, where school densities up to $614 \times 10^6$ ind. km$^{-2}$ were reported from Allen Bay (Matley et al. 2012), or benthic population abundance of 23,800 ind. km$^{-2}$ near Svalbard (Nahrgang et al. 2014). In previous studies, mainly pelagic and demersal trawls were used in open water areas (Ponomarenko 2000; Matley et al. 2013; Nahrgang et al. 2014), while under-ice abundance estimates were made based on hand net sampling (Melnikov and Chernova 2013) and observations by divers (Gradinger and Bluhm 2004). Using the SUIT enabled us to representatively capture the variability of the under-ice environment and facilitate large-scale abundance estimates of under-ice polar cod, assuming other error sources were minimal. Such error sources may be the low efficiency of the SUIT to sample animals from crevices and wedges in the ice, or the ability of polar cod to avoid or escape the net. Videos from the SUIT camera showed no indication of escape or avoidance of the net by polar cod. The mere omnipresence of polar cod in under-ice catches rather indicated that the sluggish lifestyle of polar cod (Gradinger and Bluhm 2004) may have worked in favour of sampling this species with a net that is relatively small for catching fast-swimming fish. Due to the uncertainties regarding the potential sampling of animals protected by the under-ice topography, however, the abundance estimates presented here should be regarded rather as a minimum estimate of the true abundance.

Our statistical model using purely physical variables showed that higher fish abundances were associated with lower surface salinity, thicker sea-ice and higher sea-ice coverage during sampling. Surface salinity was significantly higher in the Nansen Basin than in the Amundsen Basin due to the larger influence of Atlantic Water (Rudels et al. 2013; David et al. 2015). Besides regional differences in water mass distribution, reduced surface salinity may be caused by freshwater release of melting sea-ice. Like most stations in the Amundsen Basin, station 216 in the Nansen Basin had a relatively low surface salinity and sea-ice in an advanced state of melting (David et al. 2015), associated with comparably high abundance of polar cod (Fig. 1). Besides lower surface salinity, and probably melting conditions, modal sea-ice thickness and sea-ice coverage during sampling had a positive effect on modelled polar cod abundance. This is not a contradiction, since it implies that in areas of decaying sea-ice polar cod most likely concentrated under the remaining thicker ice. Deterioration of the sea-ice habitat and melting of ice wedges, which serve as protection for the fish, have been proposed to explain higher polar cod abundance found under the remaining sea-ice during late summer (Hop and Pavlova 2008). Clearly, the under-ice habitat was preferred to the

open water surface layer, as is evident from the positive effect of sea-ice coverage during sampling on modelled polar cod abundance.

A significant influence of melting conditions on the distribution of polar cod was confirmed by the negative effect of surface salinity in the model including prey density. The positive effect of the under-ice density of the ice-amphipod *A. glacialis* on modelled polar cod abundance indicates that under-ice prey availability was probably a key factor influencing the under-ice distribution of polar cod (Table 3). Release of ice amphipods into the pelagic habitat has been reported to occur during advanced stages of ice melt and break-up, offering a pulse of high-energy prey at the ice–water interface (Scott et al. 1999; Hop et al. 2011). The diet of polar cod under sea-ice, however, is not well documented, because the inaccessibility of this habitat has so far only allowed a small number of living fish to be analysed, leaving little evidence of polar cod feeding on sea-ice resources (Renaud et al. 2012). Polar cod collected north of the Svalbard archipelago by under-ice divers were mainly 1-year-old fish and had a diet containing *A. glacialis* and other ice amphipods among various pelagic resources (Lønne and Gulliksen 1989). Preliminary data from an analysis of 13 stomachs of polar cod collected during the present study, from seven stations, indicated that ice-associated copepods (*Tisbe* spp.) and the under-ice-amphipod *A. glacialis* were important food items (H. Flores, unpublished data).

While statistical relationships do not necessarily imply cause–effect relationships, the factors selected by the two statistical models represent plausible ecological interactions: our model results could imply that polar cod were concentrating under remaining sea-ice during advancing melt and preferred thicker sea-ice, that survived longest and was most likely to host sufficient under-ice prey.

### Population structure and allometrics

We found fish with TLs ranging between 52 and 140 mm. Their mean size was 76 mm, which corresponded to the first-year age class according to Ponomarenko (2000). This mean size is lower than previously reported mean size values for first-year fish from coastal Arctic ice-covered regions (Lønne and Gulliksen 1989), but similar to observations from the central Arctic deep-sea basins (Melnikov and Chernova 2013). The length of the first-year polar cod is related to the time of hatching and depends on the growth rate of juveniles. According to the length–age relationship $SL_{mm} = 4.357 + 0.196\ age_{days}$ described in Bouchard and Fortier (2011), these 52 to 140 mm TL polar cod were between 201 and 652 days old (mean = 336 days) in August–September. Since hatching period was recorded from January to July in the Laptev Sea (Bouchard and Fortier 2011), this suggests either the under-ice fish

represented the latest hatchers or the growth rate of under-ice fish was much slower than the pelagic ones.

The growth rate of juveniles depends on the temperature and the food availability in the environment (Ponomarenko 2000). The under-ice water temperature was below -1 °C in the Eurasian Basin, probably inducing a slower growth rate for fish associated with the sea-ice habitat compared to coastal habitats (Falk-Petersen et al. (1986). In our study, the regression coefficient *b* describing the weight–length relationship was 2.13. This value is not in line with the cubic law presumed for this relationship (Craig et al. 1982; Matley et al. 2013). This was probably due to the dominance of young fish in our samples, as in our size range, the weight–length relationship of the entire population found by Matley et al. (2013) fits still well with our data (Pearson's correlation coefficient = 0.97, $p < 0.001$). Our low values of regression coefficient *b* could mean that the young fish from our study were investing more energy in growth, and less in lipid storage, as is common in juvenile fish (Anthony et al. 2000).

The under-ice fish from our samples had very low hepatosomatic index (HSI) values compared with polar cod from the Canadian Arctic or Svalbard, which included a higher proportion of large fish (Nahrgang et al. 2010; Matley et al. 2013). The lower HSI and higher condition index (CI) values in the Nansen Basin compared to samples from the Amundsen Basin could indicate that local feeding conditions, prior to the sampling, were more favourable in the Amundsen Basin.

Somewhat contrasting with generally low HSI values, the energy content in our fish was at the high end of the range previously reported for polar cod (Hop et al. 1997a; Elliott and Gaston 2008; Harter et al. 2013), suggesting a high lipid content in tissue other than liver. In polar cod from the present study, gonads were the most lipid-rich tissue, DW lipid content averaging 87 % (D. Kohlbach, unpublished data). At the end of summer, polar cod start allocating energy to gonadal development (Hop et al. 1995). Hence, carbon resources were probably routed to gonads development rather than to storage lipids in the liver. At the end of summer, GSI values are below 5 % (Hop et al. 1995) and increase in mature polar cod to about 30 % by the spawning period in January (Hop et al. 1995; Nahrgang et al. 2014). The gonadosomatic index (GSI) values in our study (Table 5) were comparable with GSI in larger polar cod in July–August, as reported in Hop et al. (1995), indicating that fish from our study could have only begun to develop from the juvenile state towards reproductive maturity. The high-energy content found in this study for polar cod exceeds those reported by Elliott and Gaston (2008) for Canadian Arctic (21.9 kJ/g dry weight) and by Weslawski et al. (1994) for the Svalbard region (24.2 kJ/g dry weight) and is similar to those reported by

Cairns (1987) for the western Hudson Strait (26.5 kJ/g dry weight). For polar cod in the present study, accumulation of energy could have been facilitated by feeding on lipid-rich under-ice amphipods, such as *A. glacialis* and *Onisimus glacialis* (Scott et al. 1999). This highlights the potential of polar sea-ice habitats to nourish and maintain highly energy-efficient food webs.

### 'Sea-ice drift' hypothesis

Assuming that young polar cod drift passively with sea-ice, we hypothesised that the observed under-ice fish distribution in the central Arctic could be related to populations in the area of ice formation. The actual timing or mechanism determining fish to associate with sea-ice is not known. According to age estimates of fish in the present study, we consider that the latest hatchers are more likely to remain associated with the underside of sea-ice. Instead of migrating to deeper layers like other young of the year fish (Geoffroy et al. in press), this behaviour would allow them to avoid competition with older, hence bigger, individuals from the same year, or to avoid predation. During the sea-ice drift, limited mobility of the fish outside their under-ice habitat was reported (Lønne and Gulliksen 1989; Gradinger and Bluhm 2004). Only during storm events fish were observed swimming at some distance from the ice (Melnikov and Chernova 2013). When calm conditions were restored, fish seemed to seek shelter in their under-ice refuge again (Melnikov and Chernova 2013), indicating only short interruptions of their fidelity to the sea-ice underside.

To investigate pathways and formation areas of sampled sea-ice, back-tracking of sea-ice at the sampling locations was performed using a combination of NSIDC/CERSAT sea-ice drift and concentration information. We found that ice forming near Franz Josef Land and in the Kara Sea drifted into the Nansen Basin, whereas ice that formed along the western Laptev Sea coast, east of Severnaya Zemlya, drifted into the Amundsen Basin. We found higher fish abundances in the Amundsen Basin, which was linked to sea-ice originating from the Laptev Sea—Severnaya Zemlya area. If the under-ice population of polar cod in the high Arctic reflects coastal population dynamics where the sampled sea-ice was formed, then the Laptev Sea shelf, particularly in the vicinity of Severnaya Zemlya, likely served as an important recruitment ground for under-ice polar cod. Higher recruitment in that area could have been enhanced by the presence of early polynyas (Bouchard and Fortier 2008).

The accuracy of ice drift pathway estimates is, however, difficult to assess, since buoy observations of ice drift in the eastern Arctic Ocean are rare. In addition, the uncertainties associated with ice drift products are not spatially uniform (Sumata et al. 2014). For back-tracking, we therefore applied a drift dataset that shows good performance on the Siberian shelf (Rozman et al. 2011; Krumpen et al. 2013). Because CERSAT motion data are only available during winter months, the summer period (June–August) was bridged with NSIDC drift data. During summer months, however, high temperatures and strong surface melt of sea-ice make sea-ice drift determination more challenging, which may introduce additional uncertainty to our estimates of sea-ice origin and pathways.

A good agreement of the size/age structure of under-ice fish with drift times from their potential recruitment regions provides strong indication of a continuous sea-ice-driven advection of polar cod from specific coastal hatching areas across the Arctic Ocean. Spawning takes place in January and February in the Kara Sea (Ponomarenko 2000), followed by hatching usually during May and June (Ponomarenko 2000). In the Laptev Sea, hatching already starts by the end of winter and extends to July (Bouchard and Fortier 2011). According to Bouchard and Fortier (2011), larvae length in late summer can vary form 10 mm in July hatchers to 50 mm in January hatchers. By the time new sea-ice forms, generally October to December in the case of our back-tracked sea-ice, the metamorphosis is completed, but the post-larvae are typically not yet fully active swimmers. Post-larvae remaining in the surface water (Graham and Hop 1995) might seek refuge under the sea-ice and can get carried along with the sea-ice drift. Assuming a larval growth rate of 0.188 mm day$^{-1}$ for a mean under-ice temperature of $-1.5\ °C$ (growth = $0.032 \times$ temperature $+ 0.236$; Bouchard and Fortier 2011) and considering that larvae spent 120 days from summer until ice formed near coastal areas, plus around 300 days mean drift of the sampled sea-ice (Table 2), we would expect mainly first-year polar cod with TLs between about 88 and 128 mm in our under-ice catches, which agrees well with our observations. Hence, it appears realistic that young polar cod recruited to the sea-ice in the Kara and Laptev Seas and subsequently drifted into the central Arctic Ocean.

In spite of such strong circumstantial evidence, however, polar cod distribution in the central Arctic Ocean may alternatively or in combination with sea-ice drift be driven by other vectors, such as ocean currents and migration of fish that associate with the sea-ice underside at an older age.

### The ecological importance of under-ice polar cod in the central Arctic Ocean

The central role of polar cod in the Arctic marine food web is mainly related to their high standing biomass on the Arctic shelves (Hop and Gjøsæter 2013). Huge aggregations of polar cod estimated from coastal areas were found to be a sufficient energy resource to support the high abundance of

top predators reported for the same regions (Welch et al. 1992, 1993; Crawford and Jorgenson 1996; Matley et al. 2012). However, no large-scale polar cod stock estimates exist from the ice-covered central Arctic Ocean.

The mere omnipresence of polar cod we found over such vast area, even considering minimum abundances, indicates the potential of central Arctic under-ice habitats to host a significant fish stock. This stock could be indicative of a substantial trophic carbon flux in a central Arctic Ocean assumed to deliver relatively low primary productivity compared to the Arctic shelves (Fernández-Méndez et al. 2015). Spatial and seasonal heterogeneity of primary production and consumers connecting algal biomass to fish might influence fish sparse distribution.

The outcome of statistical models and high-energy content of the fish suggest that during the drift phase, polar cod were indeed closely associated with the underside of sea-ice, where they found ample high-energy food to survive the drift, until they begin their first spawning cycle. By advection with the Transpolar sea-ice Drift, juvenile polar cod hatched on the Siberian shelf could potentially recruit to populations in the Svalbard archipelago, Barents Sea and Greenland Sea, enhancing genetic exchange among polar cod populations around the Arctic Ocean. In spite of relatively low fish abundance, their omnipresence over the entire Eurasian Basin indicates that the central Arctic under-ice habitats may constitute a favourable environment for polar cod survival and a potential source of genetic exchange and recruitment for coastal populations. As the central Arctic will be exposed to further shortening of the ice-covered season and reduced sea-ice extent, it remains unclear how the under-ice subpopulation will be affected and to which extent this will impact the pan-Arctic population of polar cod.

### Compliance with ethical standards

This article does not contain any studies with human participants performed by any of the authors or any experimental studies with animals performed by any of the authors. All works were performed according to and within the regulations enforced by the German Animal Welfare Organisation, and no specific permissions were required. The R/V Polarstern is operated by Alfred Wegener Institute and has all necessary authorisation to use trawls to collect animals for scientific purposes. The organisms collected are neither protected nor endangered in the central Arctic waters.

## References

Anthony JA, Roby DD, Turco KR (2000) Lipid content and energy density of forage fishes from the northern Gulf of Alaska. J Exp Mar Biol Ecol 248:53–78. doi:10.1016/S0022-0981(00)00159-3

Barbosa AM, Brown JA, Jimenez-Valverde A, Real R (2015) modEvA: model evaluation and analysis. http://R-Forge.R-project.org/projects/modeva/

Benoit D, Simard Y, Fortier L (2008) Hydroacoustic detection of large winter aggregations of Arctic cod (*Boreogadus saida*) at depth in ice-covered Franklin Bay (Beaufort Sea). J Geophys Res Oceans. doi:10.1029/2007JC004276

Benoit D, Simard Y, Fortier L (2014) Pre-winter distribution and habitat characteristics of polar cod (*Boreogadus saida*) in southeastern Beaufort Sea. Polar Biol 37:149–163. doi:10.1007/s00300-013-1419-0

Boetius A et al (2013) Export of algal biomass from the melting Arctic sea-ice. Science 339:1430–1432. doi:10.1126/science.1231346

Bouchard C, Fortier L (2008) Effects of polynyas on the hatching season, early growth and survival of polar cod *Boreogadus saida* in the Laptev Sea. Mar Ecol Prog Ser 355:247–256. doi:10.3354/Meps07335

Bouchard C, Fortier L (2011) Circum-arctic comparison of the hatching season of polar cod *Boreogadus saida*: a test of the freshwater winter refuge hypothesis. Prog Oceanogr 90:105–116. doi:10.1016/j.pocean.2011.02.008

Bradstreet MSW, Cross WE (1982) Trophic relationships at high Arctic ice edges. Arctic 35:1–12

Brekke B, Gabrielsen G (1994) Assimilation efficiency of adult Kittiwakes and Brünnich's Guillemots fed Capelin and Arctic Cod. Polar Biol 14:279–284. doi:10.1007/bf00239177

Cairns D (1987) Diet and foraging ecology of Black guillemots in Northeastern Hudson Bay. Can J Zool 65:1257–1263

Craig PC, Griffiths WB, Haldorson L, McElderry H (1982) Ecological studies of Arctic Cod (*Boreogadus saida*) in Beaufort Sea coastal waters, Alaska. Can J Fish Aquat Sci 39:395–406. doi:10.1139/f82-057

Crawford R, Jorgenson J (1996) Quantitative studies of Arctic cod (*Boreogadus saida*) schools: important energy stores in the Arctic food web. Arctic 49:181–193

David C, Lange B, Rabe B, Flores H (2015) Community structure of under-ice fauna in the Eurasian central Arctic Ocean in relation to environmental properties of sea-ice habitats. Mar Ecol Prog Ser 522:15–32. doi:10.3354/meps11156

Elliott KH, Gaston AJ (2008) Mass–length relationships and energy content of fishes and invertebrates delivered to nestling thick-billed murres *Uria lomvia* in the Canadian Arctic, 1981–2007. Mar Ornithol 36:25–34

Falk-Petersen I-B, Frivoll V, Gulliksen B, Haug T (1986) Occurrence and size/age relations of polar cod, *Boreogadus Saida* (Lepechin), in Spitsbergen coastal waters. Sarsia 71:235–245. doi:10.1080/00364827.1986.10419693

Fernández-Méndez M, Rabe B, Katlein C, Nicolaus M, Peeken I, Flores H, Boetius A (2015) Photosynthetic production in the Central Arctic during the record sea-ice minimum in 2012.

Biogeosci Discuss 12:2897–2945. doi:10.5194/bgd-12-2897-2015

Fetterer F, Knowles K, Meier W, Savoie M (2002) Sea-ice index. monthly mean sea-ice extent. Boulder, Colorado USA: National Snow and Ice Data Center. http://dx.doi.org/10.7265/N5QJ7F7W

Flores H et al (2012) The Association of Antarctic Krill *Euphausia superba* with the under-ice habitat. PLoS One. doi:10.1371/journal.pone.0031775

Fortier L, Sirois P, Michaud J, Barber D (2006) Survival of Arctic cod larvae (*Boreogadus saida*) in relation to sea-ice and temperature in the Northeast Water Polynya (Greenland Sea). Can J Fish Aquat Sci 63:1608–1616. doi:10.1139/f06-064

Fowler C, Emery W, Tschudi M (2013) Polar pathfinder daily 25 km EASE-grid sea-ice motion vectors. Version 2. (daily and mean gridded field). Boulder, Colorado USA: NASA National Snow and Ice Data Center Distributed Active Archive Center. http://dx.doi.org/10.5067/LHAKY495NL2T

Geoffroy M, Robert D, Darnis G, Fortier L (2011) The aggregation of polar cod (*Boreogadus saida*) in the deep Atlantic layer of ice-covered Amundsen Gulf (Beaufort Sea) in winter. Polar Biol 34:1959–1971. doi:10.1007/s00300-011-1019-9

Geoffroy M, Majewski A, LeBlanc M, Gauthier S, Walkusz W, Reist JD, Fortier L (in press) Vertical segregation of age-0 and age-1 + polar cod (*Boreogadus saida*) over the annual cycle in the Canadian Beaufort Sea. Polar Biol Special 'Arctic Gadids' issue

Gjøsæter H, Prozorkevich D (2012) In: Eriksen E (Ed.) Survey report from the joint Norwegian/Russian ecosystem survey in the Barents Sea August–October 2012. IMR/PINRO Joint Report Series, no. 2/2012, pp 50–56, ISSN:1502-8828

Gradinger RR, Bluhm BA (2004) In-situ observations on the distribution and behavior of amphipods and Arctic cod (*Boreogadus saida*) under the sea-ice of the High Arctic Canada Basin. Polar Biol 27:595–603. doi:10.1007/s00300-004-0630-4

Graham M, Hop H (1995) Aspects of reproduction and larval biology of Arctic cod (*Boreogadus saida*). Arctic 48:130–135

Harter BB, Elliott KH, Divoky GJ, Davoren GK (2013) Arctic cod (*Boreogadus saida*) as prey: fish length-energetics relationships in the Beaufort Sea and Hudson Bay. Arctic 66:191–196

Haug T, Tormod Nilssen K, Lindblom L, Lindstrøm U (2007) Diets of hooded seals (*Cystophora cristata*) in coastal waters and drift ice waters along the east coast of Greenland. Mar Biol Res 3:123–133. doi:10.1080/17451000701358531

Hop H, Gjøsæter H (2013) Polar cod (*Boreogadus saida*) and capelin (*Mallotus villosus*) as key species in marine food webs of the Arctic and the Barents Sea. Mar Biol Res 9:878–894. doi:10.1080/17451000.2013.775458

Hop H, Pavlova O (2008) Distribution and biomass transport of ice amphipods in drifting sea-ice around Svalbard. Deep Sea Res Part II Top Stud Oceanogr 55:2292–2307. doi:10.1016/j.dsr2.2008.05.023

Hop H, Trudeau VL, Graham M (1995) Spawning energetics of Arctic cod (*Boreogadus saida*) in relation to seasonal development of the ovary and plasma sex steroid levels. Can J Fish Aquat Sci 52:541–550. doi:10.1139/f95-055

Hop H, Tonn WM, Welch HE (1997a) Bioenergetics of Arctic cod (*Boreogadus saida*) at low temperatures. Can J Fish Aquat Sci 54:1772–1784

Hop H, Welch HE, Crawford RE (1997b) Population structure and feeding ecology of Arctic cod schools in the Canadian High Arctic. In: Reynolds J (ed) Fish Ecology in Arctic North America, Fairbanks, Alaska, 19–21 May 1992. Am Fish Soc Symp 19, Bethesda, Maryland, pp 68–80

Hop H, Mundy C, Gosselin M, Rossnagel A, Barber D (2011) Zooplankton boom and ice amphipod bust below melting sea-ice in the Amundsen Gulf, Arctic Canada. Polar Biol 34:1947–1958. doi:10.1007/s00300-011-0991-4

IPPC (2014) Part A: global and sectoral aspects-working group II contribution to the fifth assesment report of the intergovernmental panel of climate change. In: Field CB, Barros VR, Dokken DJ, Mach KJ, Mastrandrea MD, Bilir TE, Chatterjee M, Ebi KL, Estrada YO, Genova RC, Girma B, Kissel ES, Levy AN, MacCracken S, Mastrandrea PR, White LL (eds) Climate change 2014: impacts, adaptation and vulnerability. Cambridge University Press, Cambridge, 1132 pp

Krumpen T, Janout M, Hodges KI, Gerdes R, Girard-Ardhuin F, Holemann JA, Willmes S (2013) Variability and trends in Laptev Sea-ice outflow between 1992–2011. Cryosphere 7:349–363. doi:10.5194/tc-7-349-2013

Kwok R, Rothrock DA (2009) Decline in Arctic sea-ice thickness from submarine and ICESat records: 1958–2008. Geophys Res Lett 36:L15501. doi:10.1029/2009gl039035

Lønne O, Gabrielsen G (1992) Summer diet of seabirds feeding in sea-ice-covered waters near Svalbard. Polar Biol 12:685–692

Lønne O, Gulliksen B (1989) Size, age and diet of polar cod, *Boreogadus saida* (Lepechin 1773), in ice covered waters. Polar Biol 9:187–191

Markus T, Stroeve JC, Miller J (2009) Recent changes in Arctic sea-ice melt onset, freezeup, and melt season length. J Geophys Res Oceans 114:C12024. doi:10.1029/2009jc005436

Matley JK, Crawford RE, Dick TA (2012) Summer foraging behaviour of shallow-diving seabirds and distribution of their prey, Arctic cod (*Boreogadus saida*), in the Canadian Arctic. Polar Res. doi:10.3402/polar.v31i0.15894

Matley J, Fisk A, Dick T (2013) The foraging ecology of Arctic cod (*Boreogadus saida*) during open water (July–August) in Allen Bay, Arctic Canada. Mar Biol 160:2993–3004. doi:10.1007/s00227-013-2289-2

McCullagh P, Nelder JA (1989) Generalized linear models, vol 2. Chapman and Hall London, United Kingdom

Melnikov IA, Chernova NV (2013) Characteristics of under-ice swarming of polar cod *Boreogadus saida* (Gadidae) in the Central Arctic Ocean. J Ichthyol 53:7–15. doi:10.1134/s0032945213010086

Nahrgang J, Camus L, Broms F, Christiansen JS, Hop H (2010) Seasonal baseline levels of physiological and biochemical parameters in polar cod (*Boreogadus saida*): implications for environmental monitoring. Mar Pollut Bull 60:1336–1345. doi:10.1016/j.marpolbul.2010.03.004

Nahrgang J, Varpe Ø, Korshunova E, Murzina S, Hallanger IG, Vieweg I, Berge J (2014) Gender specific reproductive strategies of an arctic key species (*Boreogadus saida*) and implications of climate change. PLoS One 9:e98452. doi:10.1371/journal.pone.0098452

Ponomarenko V (2000) Eggs, larvae, and juveniles of polar cod *Boreogadus saida* in the Barents, Kara, and White Seas. J Ichthyol 40:165–173

R Core Team (2015) R: A language and environment for statistical computing. R Foundation for Statistical Computing, Vienna, Austria. http://www.R-project.org/

Rabe B, Wisotzki A, Rettig S, Somavilla Cabrillo R, Sander H (2012) Physical oceanography during POLARSTERN cruise ARK-XXVII/3 (IceArc). Alfred Wegener Inst Helmholtz Cent Polar Mar Res Bremerhav. doi:10.1594/PANGAEA.802904

Renaud P, Berge J, Varpe Ø, Nahrgang J, Ottesen C, Hallanger I (2012) Is the poleward expansion by Atlantic cod and haddock threatening native polar cod, Boreogadus saida? Polar Biol 35:401–412. doi:10.1007/s00300-011-1085-z

Rigor IG, Wallace JM (2004) Variations in the age of Arctic sea-ice and summer sea-ice extent. Geophys Res Lett. doi:10.1029/2004gl019492

Rozman P et al (2011) Validating satellite derived and modelled sea-ice drift in the Laptev Sea with in situ measurements from the winter of 2007/08. Polar Res. doi:10.3402/Polar.V30i0.7218

Rudels B, Schauer U, Björk G, Korhonen M, Pisarev S, Rabe B, Wisotzki A (2013) Observations of water masses and circulation in the Eurasian Basin of the Arctic Ocean from the 1990s to the late 2000s. Ocean Sci Discuss 9:147–169. doi:10.5194/os-9-147-2013

Scott CL, Falk-Petersen S, Sargent JR, Hop H, Lønne OJ, Poltermann M (1999) Lipids and trophic interactions of ice fauna and pelagic zooplankton in the marginal ice zone of the Barents Sea. Polar Biol 21:65–70. doi:10.1007/s003000050335

Shaw W, Stanton T, McPhee M, Morison J, Martinson D (2009) Role of the upper ocean in the energy budget of Arctic sea-ice during SHEBA. J Geophys Res Oceans. doi:10.1029/2008JC004991

Shimada K et al (2006) Pacific Ocean inflow: influence on catastrophic reduction of sea-ice cover in the Arctic Ocean. Geophys Res Lett. doi:10.1029/2005gl025624

Snyder JP (1992) An Equal-Area Map Projection For Polyhedral Globes. Cartographica. Int J Geogr Inf Geovis 29:10–21. doi:10.3138/27h7-8k88-4882-1752

Søreide JE, Hop H, Carroll ML, Falk-Petersen S, Hegseth EN (2006) Seasonal food web structures and sympagic–pelagic coupling in the European Arctic revealed by stable isotopes and a two-source food web model. Prog Oceanogr 71:59–87. doi:10.1016/j.pocean.2006.06.001

Stroeve J, Serreze M, Holland M, Kay J, Malanik J, Barrett A (2012) The Arctic's rapidly shrinking sea-ice cover: a research synthesis. Clim Change 110:1005–1027. doi:10.1007/s10584-011-0101-1

Sumata H et al (2014) An intercomparison of Arctic ice drift products to deduce uncertainty estimates. J Geophys Res Oceans 119:4887–4921. doi:10.1002/2013jc009724

Van de Putte A, Flores H, Volckaert F, van Franeker J (2006) Energy content of Antarctic mesopelagic fishes: implications for the marine food web. Polar Biol 29:1045–1051. doi:10.1007/s00300-006-0148-z

Van de Putte AP, Jackson GD, Pakhomov E, Flores H, Volckaert FAM (2010) Distribution of squid and fish in the pelagic zone of the Cosmonaut Sea and Prydz Bay region during the BROKE-West campaign. Deep Sea Res Part II Top Stud Oceanogr 57:956–967

van Franeker JA, Flores H, Van Dorssen M (2009) Surface and Under Ice Trawl (SUIT). In: Flores H (ed) Frozen Desert alive—the role of sea-ice for pelagic macrofauna and its predators: implications for the Antarctic pack-ice food web. Dissertation, University of Groningen, Groningen, Netherlands

Vaz S, Martin CS, Eastwood PD, Ernande B, Carpentier A, Meaden GJ, Coppin F (2008) Modelling species distributions using regression quantiles. J Appl Ecol 45:204–217. doi:10.1111/j.1365-2664.2007.01392.x

Welch HE et al (1992) Energy flow through the marine ecosystem of the Lancaster sound region, Arctic Canada. Arctic 45:343–357

Welch HE, Crawford RE, Hop H (1993) Occurrence of Arctic cod (Boreogadus saida) schools and their vulnerability to predation in the Canadian High Arctic. Arctic 46:331–339

Weslawski JM, Ryg M, Smith TG, Oritsland NA (1994) Diet of ringed seals (Phoca hispida) in a fjord of West Svalbard. Arctic 47:109–114

Wilcoxon F (1945) Individual comparisons by ranking methods. Biometrics Bulletin 1:80–83